DAD Post-Tensioned Concrete Connections with Lead Dampers: Analytical Models and Experimental Validation

Geoffrey W. Rodgers, J. Geoffrey Chase

Department of Mechanical Engineering, University of Canterbury, New Zealand

J. B. Mander

Department of Civil Engineering, Texas A&M University, College Station, TX, USA

Rajesh P Dhakal, and Kevin M Solberg

Department of Civil Engineering, University of Canterbury, New Zealand

ABSTRACT:

Jointed precast concrete systems typically have low inherent damping and are thus well suited for the use of supplemental damping systems. This work examines the analytical modeling and experimental validation of full-scale beam-column connections constructed utilising Damage Avoidance Design (DAD) principles with un-bonded post-tensioned tendons and rocking interfaces. These test articles also utilise high force-to-volume extrusion-based energy dissipaters to provide supplemental energy dissipation and modify joint hysteretic performance. Independently validated analytical models of both the joint and devices are combined to create a full system model. In particular, analytical modelling is utilised to characterise the damper augmented beam-to-column rocking connections, using a rate-dependent tri-linear compound version of the well-known Menegotto-Pinto rule. The analytical model is verified against a number of experimental results over inter-story drifts of 1-4%. The relative contributions to the overall force-displacement behaviour of the structural, post-tensioning and damper elements are also delineated, indicating the significant role of the damping devices in mitigating structural response energy. Overall, the precast system behaviour is improved by the addition of the extrusion based damping system, showing increases in hysteretic energy dissipation of up to 300% while maintaining static re-centring capability.

1 INTRODUCTION

Earthquakes can cause significant damage and degradation, especially in beam/column connections. Current capacity design for monolithic reinforced concrete structures provides ductility by localising inelastic behaviour to specific regions called plastic hinge zones. Although plastic hinge damage provides significant energy dissipation during the event and provides adequate life safety, it is desirable to achieve these objectives without permanent structural damage. The use of rocking connections and, in particular, joints designed using the emerging Damage Avoidance Design (DAD) philosophy (Li 2006, Solberg 2007), enables the structure to undergo inelastic hysteretic response without notable structural damage. This new design philosophy enables structures to be constructed that not only protect life safety, but also address the large financial cost of earthquake damage.

Jointed precast concrete systems conforming to DAD typically have low inherent damping. They are thus well suited for supplemental damping systems. Recently, considerable attention has focused on yielding steel fuse-bars to provide hysteretic energy dissipation and modify overall joint hysteresis (Li, 2006; Solberg 2007). Concomitantly, research into extrusion-based damping devices has resulted in the development of high force-to-volume lead extrusion dampers (Rodgers et al 2006a,b). These dampers provide equivalent or higher forces than yielding steel fuses, and do so on every response cycle. They are also sufficiently compact to allow placement directly into structural connections.

This research outlines the experimental testing and analytical modelling of a prototype jointed precast beam-to-column sub-assemblage detailed according to the DAD philosophy. To supplement the damping, the specimen was fitted with high force-to-volume lead extrusion dampers. The primary focus is the effect of these dampers on the overall joint hysteresis. Analytical modelling of the experimental results utilises a compound rate-dependent version of the Menegotto-Pinto rule. The resulting experimentally validated model will enable easy consistent implementation design, when used in conjunction with spectral analysis-based design guidelines (Rodgers et al 2007).

2 EXPERIMENTAL INVESTIGATION

The prototype ten-storey reinforced concrete frame has three 10m bays in each direction, commonly known as the "red book" building (Bull and Brunsdon, 1998). It was designed to the New Zealand concrete standard (NZS:3101, 1995) for intermediate soil (NZS4203, 1992). Keeping all other variables constant, the same structure was designed according to DAD principles, resulting in precast beams and columns being connected via a post-tensioning system. It also has precast floor units seated on the transverse beams, leaving the longitudinal beams to resist predominately seismic forces.

An exterior joint on the second floor of 500 kN-m moment capacity was chosen for testing a 3D beam-column sub-assemblage. Using constant stress and strain similitude, the specimen was scaled to 80% full size, and consists of two beams in the longitudinal direction, and one beam in the transverse direction. The longitudinal and transverse beams are dominated by seismic and gravity loads and are referred to as the east-west seismic and north-south gravity beams, respectively. Figure 1 shows a photograph and experimental schematic. An initial 400kN axial post-tensioned prestress is provided by two 26.5mm diameter high-strength thread-bars placed in 50mm PVC ducts.

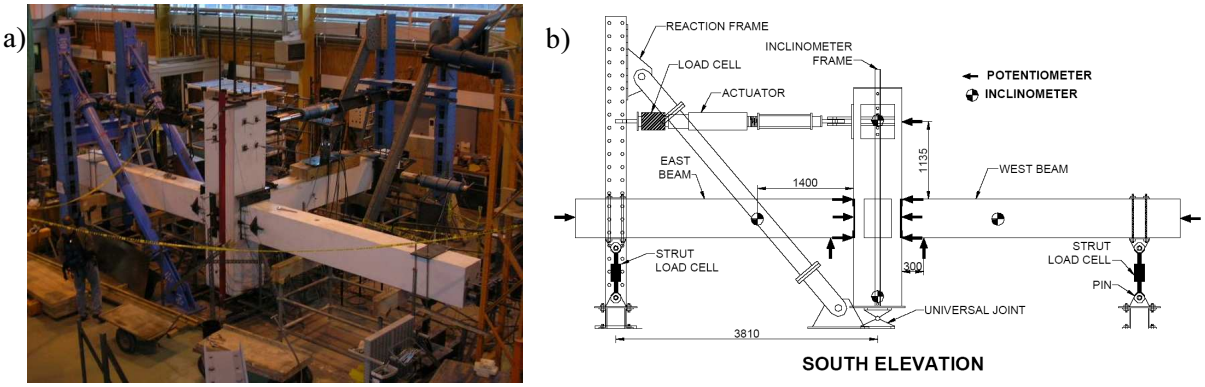

Figure 1: a) Photograph of test specimen, and b) Schematic south elevation of test setup

The tendon profile in the east-west direction utilises a straight coupler system where the tendons were pre-bent at the joint end to a radius of 1.8m. The tendons exit through the column face at the top of the beam-column interface. Straight fuse bolt-bars run at an angle through the column, with a sacrificial fuse diameter machined to 75% of the effective area to localise any inelastic tendon behaviour. A detailed schematic for the east-west connection is presented in Figure 2.

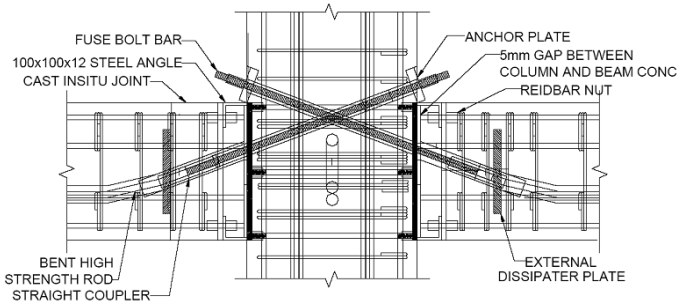

Figure 2: Post-tensioning detail at the beam-column joint in the East-West seismic direction. (Solberg, 2007)

The supplemental damping system consists of two 120kN lead-extrusion dampers mounted externally to each seismic beam, as shown in Figure 3a. Figure 3b shows the hysteresis loop for the lead extrusion dampers. Only uni-direction testing in the east-west seismic direction is considered to evaluate the impact of these devices with further experimental details in Solberg (2007).

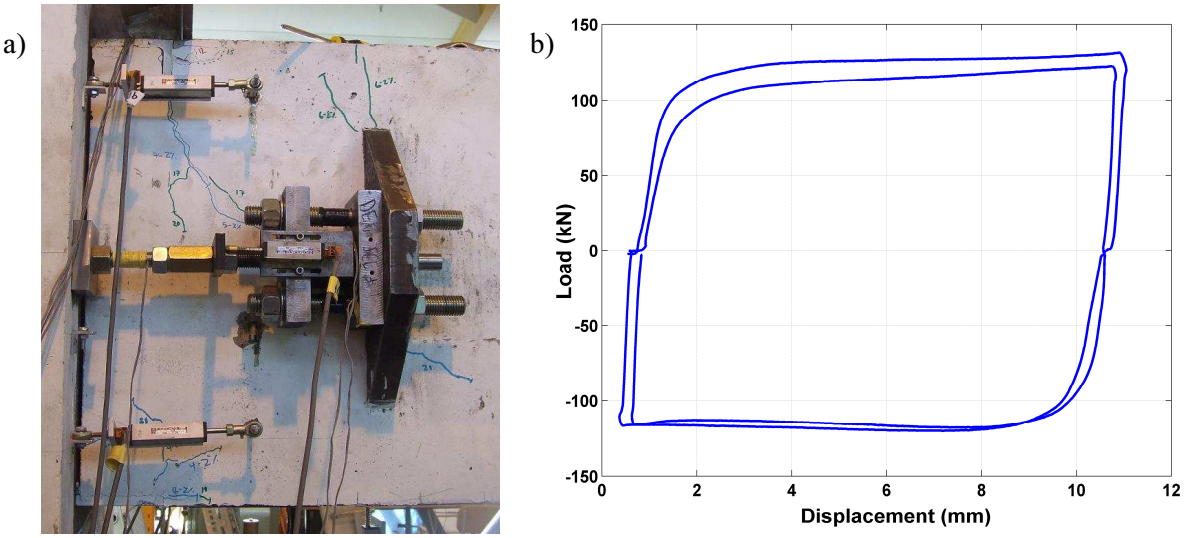

Figure 3: a) Lead extrusion damper externally mounted to the seismic beam, and b) hysteresis loop for the damper shown in a).

3 MODELLING OF OVERALL JOINT HYSTERESIS

The overall joint hysteresis, in particular the column base-shear vs lateral deflection curve, can be modelled as a combination of elastic member deflection and rigid body rotation. Initially, the presence of post-tensioning will delay gap opening and lateral column deflection will be a function of elastic deformation of the prestressed concrete elements only. This elastic deformation regime continues until the applied moment created by the lateral loading of the column exceeds the moment preventing gap opening that is provided by the post-tensioned tendons and supplemental damping system. The column base-shear required for gap opening is therefore a function of the level of prestress provided by the tendons, and the resistive force provided by the dampers.

Upon gap opening, the prestressing tendons elongate elastically along with deformation of the supplemental damping system. Further lateral deflection is then a combination of further elastic deformation of the sub-assembly, and rigid body rotation associated with joint opening. The column base-shear associated with this deflection can be calculated using beam bending theory and rigid body mechanics. The post gap-opening stiffness continues until the tendon elongation associated with the rigid body component reaches tendon yield. At this point, further column deflection, and consequently column drift, occurs with no further increase in column base-shear.

The lead extrusion dampers are modelled as non-linear velocity dependent viscous dampers (Rodgers et al 2006a,b). The stiffness of the rods connecting the dampers to the column is assumed to be rigid. Thus, any damper motion due to joint opening occurs only in the device itself. Therefore, the dampers take effect at the initiation of joint opening.

The combination of pre gap-opening elastic member deformation, post gap-opening deformation resulting in elastic tendon elongation, and post gap-opening deformation with inelastic tendon elongation creates an overall tri-linear hysteretic response. However, the smooth non-linear experimental behaviour can be more accurately modelled using a compound, rate dependent version of the Menegotto-Pinto (1973) Hysteresis rule, defined (Li, 2006):

$$F = \frac{(K_2 - K_1)\theta}{\left(1 + \left|\frac{K_1\theta}{F_p + F_D \operatorname{sgn}(\dot{x})}\right|^{\beta}\right)^{\frac{1}{\beta}}} + \frac{K_2\theta}{\left(1 + \left|\frac{K_2\theta}{F_y + F_D \operatorname{sgn}(\dot{x}) - (F_p + F_D \operatorname{sgn}(\dot{x})(1 - K_2/K_1))}\right|^{\gamma}\right)^{\frac{1}{\gamma}}} \quad (1)$$

where K_1 = stiffness of the sub-assembly during initial pre-gap-opening elastic deformation; K_2 = stiffness of the sub-assembly during post gap-opening deflection before tendon yield; θ = the drift angle of the column, $\dot{x}$ = the velocity of the damper shaft, corresponding to the velocity of the joint opening at beam centreline; where when $\dot{x} > 0$, sgn($\dot{x}$) = 1, and when $\dot{x} < 0$, sgn($\dot{x}$) = -1; F_p = column base-shear required to overcome the resistance to joint opening from prestress alone; F_y = column base-shear required to open gap to prestress tendon yield; β = exponent governing the degree of curvature that joins the tangents between the first and second linear sections of the hysteresis loops; and γ = exponent governing the degree of curvature between the second and third linear sections of the hysteresis loop, where large exponents give sharper corners closer to the tri-linear behaviour. Finally, F_D = column base shear required to overcome the lateral resistance of the subassembly due to the damper force, F_{damper}, defined (Rodgers, 2006a; Pekcan 199):

$$F_{damper} = C_\alpha |\dot{x}|^{\alpha} \operatorname{sgn}(\dot{x}) \quad (2)$$

where C_α = damper constant determined by testing at a reference velocity before installation into the joint; $\dot{x}$ = the velocity of the damper shaft; α = velocity co-efficient (constant), having a value of 0.12 (Rodgers et al, 2006a); and sgn($\dot{x}$) is as defined previously.

The initial system stiffness K_1 can be derived using moment-area theorems (Li, 2006):

$$K_1 = \frac{12(EI^*_{beam})/L_b^3}{\left(\frac{L_{col}}{L}\right)^2 + \left(\frac{L_{col} - D}{L_b}\right)^3 \left(\frac{EI^*_{beam}}{EI^*_{col}}\right)} \quad (3)$$

where EI^*_{beam} and EI^*_{col} are the effective beam and column rigidities; L_b = length of the precast beams; L = clear length between column centerlines; L_{col} = column height; and D = beam depth.

Following gap opening, the second stiffness K_2 is defined (Li, 2006):

$$K_2 = \left(\frac{L}{L_b}\right)^2 \left(\frac{D}{L_{col}}\right)^2 \frac{K_{bolt} K_{ps}}{K_{bolt} + K_{ps}} \quad (4)$$

where $K_{bolt} = A_{bolt}E_{ps}/l_{bolt}$ is the stiffness of the bolt (fuse) bar, where A_{bolt} = area and l_{bolt} = length of the fuse portion of the bolt bar. Similarly, in Equation (4), $K_{ps} = A_{ps}E_{ps}/l_{ps}$ is the stiffness of the prestressing tendon in the precast beam, where E_{ps} = Young's modulus; A_{ps} = cross-sectional area, and l_{ps} = length of the prestressing tendon in the beam.

The lateral load resistance of the subassembly with both prestressing and energy dissipaters can be evaluated by considering rigid body kinematics. Assuming the neutral axis depth is small enough to be neglected and the horizontal force component from the threaded bolt bars is equal to the prestressing force in the bolt bars, joint equilibrium gives (Li, 2006):

$$F_p = \left(P^-_{ps}\frac{e}{D} + P^+_{ps}\left(1 - \frac{e}{D}\right)\right)\cos\alpha \frac{D}{L_{col}}\frac{L}{L_b} \quad (5)$$

where P^-_{ps} and P^+_{ps} are the total tendon force in the precast beam when rocking along the bottom and top edges respectively; e = eccentricity of prestressing tendon at column face, α = angle of the

threaded fuse-bolt bars; and D, L, and L_b are defined previously. Similarly, when considering the influence of the lead extrusion damper on the subassembly:

$$F_D = F_{damper} \frac{D}{L_{col}} \frac{L}{L_b} \tag{6}$$

where F_{damper} is defined in Equation (2). Finally, the lateral strength at yielding of the sub-assembly is given by (Li, 2006):

$$F_{p\ yield} = P_{ps\ yield} \cos\alpha \frac{D}{L_{col}} \frac{L}{L_b} \tag{7}$$

where $P_{ps\ yield}$ = yield strength of fuse bolt bars.

4 EXPERIMENTAL TEST RESULTS AND DISCUSSION

4.1 Exterior Joint Results

The experimental specimen was subjected to uni-directional displacement-controlled tests representing fully reversed sine wave profiles for story drifts of 0.25, 0.5, 1 and 2%. The specimen underwent two fully reversed cycles at each drift level. At 0.25% drift, the joint remained closed, with only elastic column deflection. Minimal joint opening was observed at the 0.5% drift cycles, and notable joint opening was achieved at the 1 and 2% cycles. Movement of the column base pin due to flexibility in the connection to the strong floor resulted in apparent hysteresis near the origin, however this effect was deemed due to this flexibility and does not represent a contribution to the overall joint hysteresis.

The hysteresis loops from the experimental specimen when subjected to cycles of 1 and 2% drift are presented in Figure 4. Figure 4 also shows the theoretical result predicted by the compound, rate dependent Menegotto-Pinto equation defined in Equation (1). The model shows good agreement with the experimental results.

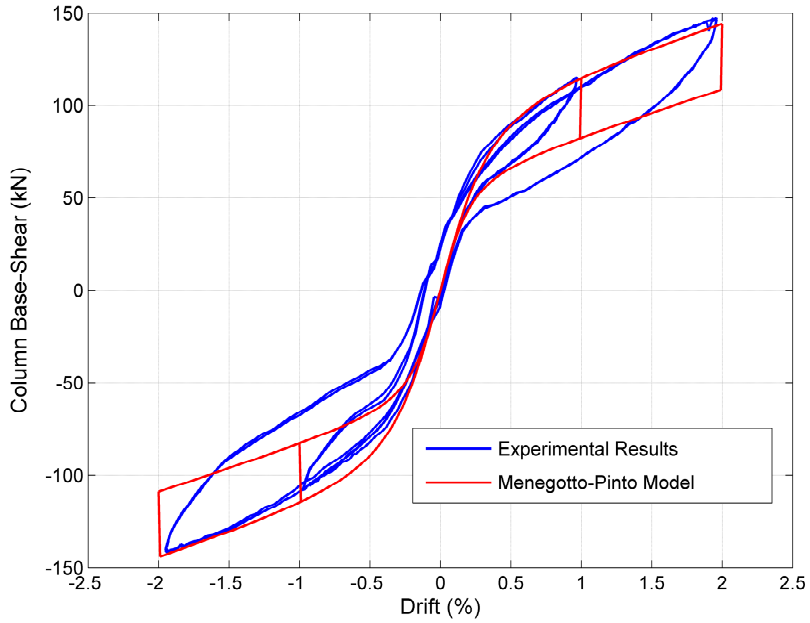

Figure 4: Experimental and analytical model results for prototype joint subjected to cycles at 1 and 2% drift.

The key differences observed in Figure 4 are a slight under-prediction in enclosed hysteretic area from the Menegotto-Pinto model, and that the theoretical loops also show over-prediction in the magnitude

of the change in force that occurs at the peak drift points. The experimental results show a gradual change in force due to flexibility of the damper shaft and connecting elements, compared to the analytical model which predicts a sharper change.

Better agreement at the extremes of the loop could be obtained by incorporating a spring in series with the damper to account for flexibility in the damper mounts and connecting rods. Thus, the contribution of the damper to the overall model has been modified such that the damper force is now defined:

$$F_{damper\,new} = \min\begin{cases} K_{connections} e_{dissipators} \theta_{connection} \\ F_{damper} \end{cases} \tag{8}$$

where $F_{damper\,new}$ = the new damper force including the effects of connection flexibility; $K_{connections}$ = the effective spring stiffness of the damper shaft and connecting elements; $e_{dissipators}$ = the eccentricity of the dampers from the rocking edge; $\theta_{connection}$ = the connection rotation due to only the rigid body rotation component of drift; and F_{damper} = the damper force as defined by Equation (2). It is important to note that new damper force, $F_{damper\,new}$, must again be modified by Equation (6) to obtain the force F_D to input into the Menegotto-Pinto model of Equation (1).

The hysteresis loops from this updated Menegotto-Pinto model using Equation (8) are presented with the experimental results in Figure 5. Much better agreement with the experimental results is seen in the regions around peak drift compared to Figure 4. Thus, the model is a better predictor of experimental behaviour.

The primary focus of this paper is on the contribution of the damping system and associated modelling, so only the uni-directional test results are presented within this paper. Full bi-directional joint characterisation details can be found in the extended works of Li (2006) and Solberg (2007).

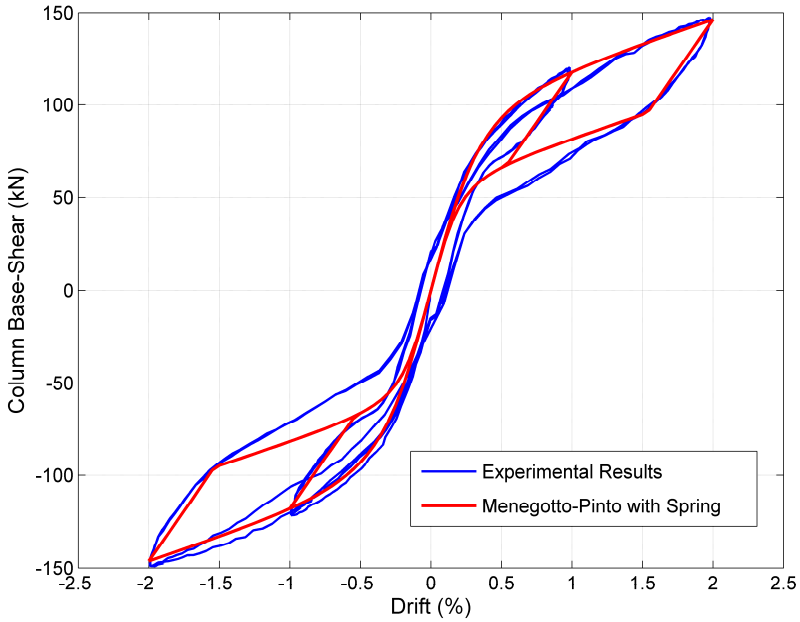

Figure 5: Menegotto-Pinto model modified to incorporate the effect of flexibility in damper connections

4.2 **Corner Joint Results**

The design force of 120kN for the lead extrusion dampers was a conservative choice from a design standpoint. The key motivation was to maintain a large factor of safety against the loss of overall joint recentring. If the resistive force provided by the dampers exceeds the prestress force then the joint

could be at risk of losing the ability to self-centre following an earthquake.

After performing numerous tests on the initial test specimen, the east beam was removed from the test set-up, and both of the dampers placed on the west beam to double the damping force. This new set-up represents a corner joint for the building, and undertaking testing with this set-up allows the recentring limit to be experimentally investigated. It is important to note that a breach of the recentring limit represents the requirement of an external force to re-centre the joint, and is shown in a hysteresis loop by a zero-force crossing of the horizontal axis at a non-zero displacement value.

Furthermore, it was of particular interest in this comparison to investigate the contribution that the supplemental damping system contributed to the overall joint hysteresis. Therefore, testing was performed on the joint with and without the dampers attached to indicate the hysteresis loops that are obtained for these two configurations. Testing was again limited to uni-directional displacement inputs for these configurations as no damping system was applied to the north-south gravity beam, rendering it unimportant here. The peak drift for the displacement inputs was increased to 4%, but two fully reversed cycles at each drift increment are used to investigate repeatability and the effect of any inelastic tendon behaviour. Results for 1, 2, 3, and 4% drifts, with and without dampers are presented in Figure 6.

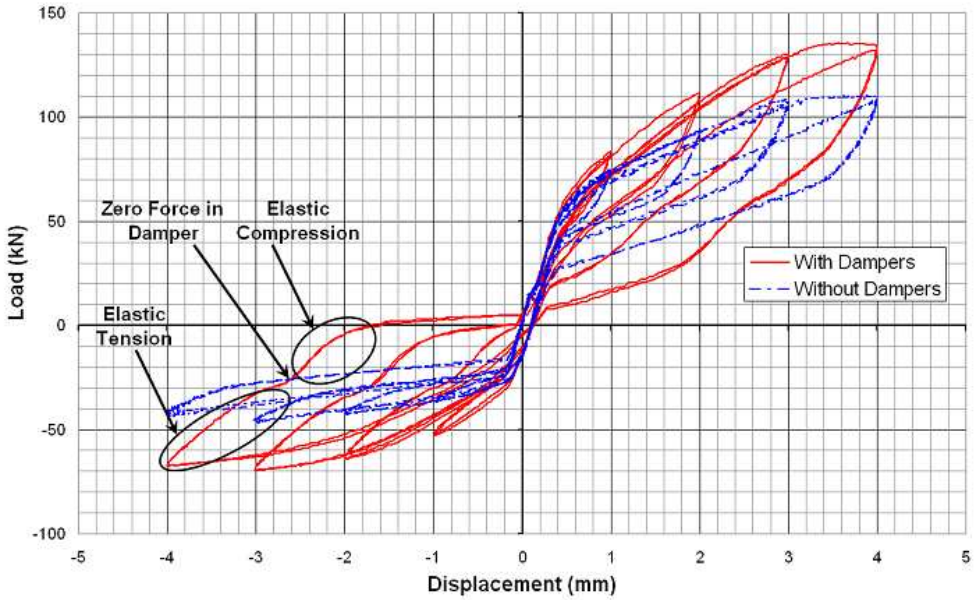

Figure 6: Comparison of joint hysteresis with and without dampers for corner joint set-up with increased damping for loading at 1, 2, 3, and 4% drift.

The first notable observation is that the hysteresis loop is asymmetric. This phenomenon can be attributed to the fact that the post-tensioning tendon arrangement of the prototype has the tendons eccentrically placed relative to the beam centreline at the beam-column interface, as shown in Figure 2. Although this eccentricity has always been present, the loops presented in Figures 4-5 do not show this asymmetry, as the presence of both the east and west beams balanced out this effect. Although the forces at each interface were asymmetrical, the west interface was undergoing the opposite joint rotation to the east interface, resulting in overall symmetry of the hysteresis loops. The removal of the east beam removed this cancellation, resulting in the asymmetric results of Figure 6.

As expected, the overall joint hysteresis loops are substantially larger when the dampers are present. Interestingly, the area enclosed within the hysteresis loops for the joint without dampers shows large disparity between the two directions. Again, this phenomenon can be traced back to the tendon profile. The inherent hysteresis for the joint without dampers is related primarily to the friction between the prestressing tendons and the PVC tube in which they are contained. The bent tendon arrangement

results in notable friction between the tendon and PVC duct as the tendon undergoes deformation from gap opening. The curve of the tendon naturally results in higher friction for gap-opening in one direction than the other.

Another important observation is the loss of recentring ability for the joint at 4% drift, as seen by the crossing of the horizontal axis at a non-zero displacement. Although the recentring capability is lost, it is only lost for negative drift angles at the largest expected (failure) drift of 4%. Importantly, the external force required to recentre the joint was a relatively minimal 5 kN. This result indicates that using this level of damping would be slightly beyond the upper limit that should be incorporated in design if such very large drifts are expected in anything but the worst case.

Finally, Figure 6 indicates that the effect of connecting rod and damper mount flexibility has a notable effect on the overall hysteretic response. At peak drift, the connecting rods to the dampers are in a state of elastic tension due to the load they are carrying. Immediately after peak drift the connecting rods must undergo a period of reduction in elastic tension before then undergoing elastic compression before the damper can provide energy dissipation. The effects of this flexibility can be clearly seen in Figure 6, where as well as this elastic deformation, there is an inflection point where some take-up can be observed in the damper mounts. These factors all slightly reduce the effectiveness of the dampers, and designers would be advised to use as stiff as practicable connecting rods and mounting plates.

The efficiency of the dampers is significantly reduced by the flexibility of the damper mounts, but significant increase in absorbed hysteretic energy is achieved when compared to the joint without dampers. In particular, for the 4% drift cycles in the negative drift direction, the enclosed hysteretic energy with the dampers is over 400% of the hysteretic area of the joint itself, indicating an increase in energy absorbed of 300%, with only minimal effects on the ability of the joint to statically re-centre.

5 CONCLUSIONS

Overall, the high force to volume lead extrusion dampers utilised here have several key benefits when compared to the use of yielding steel dissipaters. The controlled deformation within the damper enables elastic design of all connecting rods, eliminating all potential of low-cycle fatigue present with yielding steel. Second, these lead extrusion dampers provide consistent force on every (repeated) cycle, rather than only during larger cycles that induce (added) yielding. They thus provide far greater energy dissipation over an entire event than the mere comparison of 1-2 cycles done here would indicate. Third, these devices do not suffer the buckling issues that are also present with yielding steel fuse designs. All of these advantages result in more consistent, repeatable and damage free joint behaviour, as the dampers would also not require inspection or replacement after a large earthquake.

The use of a compound, rate dependent version of the Menegotto-Pinto hysteresis rule provides a compact and satisfactory method of modelling joint performance. The model slightly under-predicts the enclosed hysteretic area when compared to the experiments, but this difference can be accounted for by including the effects of tendon friction in the ducts. This anomaly is particularly obvious here due to the large friction as a result of the bent tendon design of this experimental joint. A straight tendon profile could be expected to exhibit much lower inherent damping, where model results would more accurately represent the joint behaviour, but is left to future work in this instance.

The area enclosed within the loops is slightly over-predicted near peak drifts using the model that does not allow for elastic deformation of the connecting rods and any deformation or slip in damper mounts. The modified model that accounts for these flexibility effects shows much better agreement to the experimental results in the regions near the peak drift.

Testing of a full-scale corner joint, with only one seismic beam revealed the presence of response asymmetry, both in the magnitudes of the column base-shear during deformation, and in the amount of inherent damping within the joint. These factors relate to the bent tendon profile, and were cancelled in the presence of an opposing beam. The use of lead extrusion dampers in place of yielding steel dissipaters provides more repeatable joint behaviour and eliminates low-cycle fatigue issues. In general, absorbed hysteretic energy for jointed beam-to-column connections can be increased over 300% with only minimal effects on the static recentring ability. The use of lead extrusion dampers to

provide supplemental damping has been successfully demonstrated.

The overall outcome complies with the general tenets of Damage Avoidance Design and represents a significant way forward for this type of connection. In particular, the results indicate the feasibility of this novel high force to volume damper in realistic structural connections. The experimentally validated model presented thus provides the pathway for ready implementation design in conjunction with previously developed spectral analysis based design guidelines.

ACKNOWLEDGEMENTS

Funding for this research was provided in part by the Tertiary Education Commission (TEC) through a Top Achiever Doctoral Scholarship. Funding from the Foundation for Research, Science and Technology (FRST), under the "Future Buildings" program is also gratefully acknowledged.

REFERENCES:

Bull, D., and Brunsdon, D. (1998). Examples of Concrete Structural Design to the New Zealand Standard Code of Practice for the Design of Concrete Structures-NZS3101. Cement and Concrete Association of New Zealand (CCANZ), Wellington, New Zealand.

Li, L (2006) "Further Experiment on Damage Avoid Design of Beam-to-Column Joint" Master of Engineering (ME) Thesis, Dept of Civil Engineering, University of Canterbury, Christchurch, New Zealand.

Menegotto, M. and Pinto, P.E. (1973). Method of analysis for cyclically loaded reinforced concrete plane frames including changes in geometry and non-elastic behavior of elements under combined normal force and bending. IABSE Symposium on the Resistance and Ultimate Deformability of Structures Acted on by Well-defined Repeated Loads, Lisbon.

Pekcan, G., Mander, J. B., and Chen, S.S. (1999). "Fundamental Considerations for the Design of Non-linear Viscous Dampers." Earthquake Engineering and Structural Dynamics 28: 1405-1425.

Rodgers, GW, Denmead, C, Leach, NC, Chase, JG. Mander, JB, (2006a) "Spectral evaluation of high force-volume lead dampers for structural response reduction," Proceedings New Zealand Society for Earthquake Engineering Annual Conference, Napier, New Zealand, March 10-12.

Rodgers, GW, Denmead, C, Leach, NC, Chase, JG. Mander, JB, (2006b) "Experimental development and analysis of a high force/volume extrusion damper," Proceedings New Zealand Society for Earthquake Engineering Annual Conference, Napier, New Zealand, March 10-12.

Rodgers, GW, Mander, JB, Chase, JG**,** Leach, NC, and Denmead, CS (2007). "Spectral Analysis and Design Approach for High Force-to-Volume Extrusion Damper-based Structural Energy Dissipation," Earthquake Engineering & Structural Dynamics (EESD), In Press.

Solberg, KM, (2007) "Experimental and Financial Investigations into the further development of Damage Avoidance Design" Master of Engineering (ME) Thesis, Dept of Civil Engineering, University of Canterbury, Christchurch, New Zealand.

Standards New Zealand. (1995) - NZS 3101: Part 1: 1995: Concrete Structures Standard, Standards New Zealand, Wellington.

Standards New Zealand. (1992) - NZS 4203: 1992: Code of Practice for General Structural Design, and Design Loadings for Building. Standards New Zealand, Wellington.